PHA-680632, a Novel Aurora Kinase Inhibitor with Potent Antitumoral Activity

Chiara Soncini, Patrizia Carpinelli, Laura Gianellini, Daniele Fancelli, Paola Vianello, Luisa Rusconi, Paola Storici, Paola Zugnoni, Enrico Pesenti, Valter Croci, Roberta Ceruti, Maria Laura Giorgini, Paolo Cappella, Dario Ballinari, Francesco Sola, Mario Varasi, Rodrigo Bravo, and Jürgen Moll

Abstract

Purpose: Aurora kinases play critical roles during mitosis in chromosome segregation and cell division. The aim of this study was to determine the preclinical profile of a novel, highly selective Aurora kinase inhibitor, PHA-680632, as a candidate for anticancer therapy.

Experimental Design: The activity of PHA-680632 was assayed in a biochemical ATP competitive kinase assay. A wide panel of cell lines was evaluated for antiproliferative activity. Cell cycle analysis. Immunohistochemistry, Western blotting, and Array Scan were used to follow mechanism of action and biomarker modulation. Specific knockdown of the targets by small interfering RNA was followed to validate the observed phenotypes. Efficacy was determined in different xenograft models and in a transgenic animal model of breast cancer.

Results: PHA-680632 is active on a wide range of cancer cell lines and shows significant tumor growth inhibition in different animal tumor models at well-tolerated doses. The mechanism of action of PHA-680632 is in agreement with inhibition of Aurora kinases. Histone H3 phosphorylation in Ser^{10} is mediated by Aurora B kinase, and our kinetic studies on its inhibition by PHA-680632 *in vitro* and *in vivo* show that phosphorylation of histone H3 is a good biomarker to follow activity of PHA-680632.

Conclusions: PHA-680632 is the first representative of a new class of Aurora inhibitors with a high potential for further development as an anticancer therapeutic. On treatment, different cell lines respond differentially, suggesting the absence of critical cell cycle checkpoints that could be the basis for a favorable therapeutic window.

Mitosis is a highly dynamic phase of the cell cycle and any error can have dramatic consequences as seen in most tumors, which bear chromosomal anomalies and are often aneuploid. Due to its high complexity, mitosis needs stringent regulators, among which are the Aurora kinases. Aurora proteins belong to a small family of serine/threonine kinases that are key regulators of different steps in mitosis and meiosis (for review, see refs. 1, 2). In mammalians, the Aurora family consists of three members: Aurora A, Aurora B, and the less well characterized Aurora C, whereas in yeast only one Aurora kinase gene exists. All Aurora kinases bear a conserved COOH terminus that contains the typical catalytic subdomains of a serine/threonine kinase and a destruction box that might be important for protein degradation (3–6).

Authors' Affiliation: Nerviano Medical Sciences S.r.l.-Oncology, Milan, Italy
Received 9/7/05; revised 4/20/06; accepted 4/24/06.
The costs of publication of this article were defrayed in part by the payment of page charges. This article must therefore be hereby marked *advertisement* in accordance with 18 U.S.C. Section 1734 solely to indicate this fact.
Note: Supplementary data for this article are available at Clinical Cancer Research Online (http://clincancerres.aacrjournals.org/).
Requests for reprints: Jürgen Moll, Nerviano Medical Sciences S.r.l.-Oncology, Via Pasteur 10, I-20014 Nerviano, Milan, Italy. Phone: 39-331-58-1396; Fax: 39-331-58-1374; E-mail: jurgen.moll@nervianoms.com.

doi:10.1158/1078-0432.CCR-05-1964

Despite these similarities, the three mammalian Aurora kinases show differences in subcellular localizations, timing of activation, and functions during mitosis. For example, whereas Aurora A and B mRNA and protein levels as well as kinase activity increase during mitosis, the peak of Aurora A activity is seen during prometaphase, whereas Aurora B is most active from metaphase to telophase (7).

Aurora A localizes to centrosomes during interphase and moves to the spindle poles during early mitosis. In contrast, Aurora B is a chromosomal passenger protein, where it is in a complex with at least three other chromosomal passenger proteins: inner centromere protein, survivin, and the recently described Borealin (8).

Several studies in different organisms show a role of Aurora A in centrosome maturation and spindle assembly. On the contrary, Aurora B is part of the spindle checkpoint regulating chromosome cohesion and bipolar attachment of microtubules. In addition, Aurora B has been proposed to play a role in the control of cytokinesis (9–11). Aurora C has been reported to be localized at the centrosomes and to have a limited expression in testis and in some cancer cell lines (12). However, a recent publication indicates a novel role for Aurora C, more similar to Aurora B (13). Since their discovery, Aurora kinases have been implicated in cancer and tumorigenesis (14). Initially, Aurora A and B were found to be overexpressed in primary tumors of breast and colon. Further studies revealed Aurora A amplification or overexpression in many other tumor types (15–21).

Moreover, their genetic localizations (Aurora A, 20q13; Aurora B, 17q13) map to chromosomal loci frequently altered in tumors.

Aurora A has been shown to act as an oncogene because overexpression of wild-type Aurora A or of a constitutive active mutant transforms Rat1 and NIH 3T3 cells leading to colony formation in soft agar assays (7, 22). In addition, NIH 3T3 cells expressing constitutively active Aurora A can grow as solid tumors when injected into *nu/nu* mice (7). When Aurora A is overexpressed in the diploid human breast cell line MCF10A, centrosome abnormalities and aneuploidy are observed (22). A direct role of Aurora B or C in tumorigenesis is less well documented, although Aurora B is also overexpressed in many human tumors. Aurora kinases, by virtue of their roles in mitosis, have been implicated in the genetic instability of tumor cells by controlling chromosomal ploidy.

Some of the known substrates or interacting proteins of Aurora kinases, such as Ras-GAP (23), p53 (24–26), Cdc20 (27), or NM23-H1 (28), could be important mediators in malignant transformation.

These properties make the Aurora kinases attractive targets for anticancer therapy; indeed, the first inhibitors have entered the clinic (29). At present, there are three small molecules inhibiting Aurora kinases (for review, see ref. 30) described in more details in the literature [Hesperadin (31), ZM447439 (32, 33), and VX-680 (34)] and other compounds are in development.

We report here the characterization of a novel, highly selective Aurora kinase inhibitor, which is active on a wide range of cancer cell lines *in vitro* and shows significant tumor growth inhibition (TGI) in different animal tumor models. The molecular mechanism of action of our inhibitor is in agreement with inhibition of Aurora A and B kinases as has been shown *in vitro* and *in vivo*, monitoring phosphorylation of Aurora A as well as histone H3 and BubR1. The differences in cellular response of different cell lines (e.g., some tumor cells versus normal cells) observed after treatment with this inhibitor might be due to the absence of critical cell cycle checkpoints in some tumor cells and could form the basis for a favorable therapeutic window.

Materials and Methods

Cell culture. HeLa cells (European Collection of Cell Culture, Salisbury, United Kingdom) were cultured in MEM supplemented with heat-inactivated 10% FCS. A2780 and HL60 cells (European Collection of Cell Culture) were maintained in RPMI with 10% FCS. HCT116 cells (American Type Culture Collection, Manassas, VA) were maintained in McCoy's medium with 10% FCS. U2OS cells (American Type Culture Collection) were grown in DMEM with 10% FCS. Normal human dermal fibroblasts (NHDF; Promocell, Heidelberg, Germany) were maintained in fibroblast basal medium supplemented with growth factors and with 10% FCS. Total WBC from peripheral or marrow blood of leukemia patients were purified by ACK lysis or Ficoll (Amersham, Biosciences, Pittsburgh, PA) gradients and assayed for cell viability before treatment. These samples were used after patient consent. In all the experiments, cells were treated with PHA-680632 at the indicated concentrations and times, starting from a stock solution of 10 mmol/L in DMSO (Sigma, St. Louis, MO). Nocodazole (Sigma) was used at 75 ng/mL for 9 hours.

Recombinant protein production. The coding sequences of human Aurora kinases (A, B, and C) were amplified by PCR and introduced into plasmid pDONOR201 using Gateway Cloning Technology (Invitrogen, Carlsbad, CA) and subsequently cloned into the vector PVL1393 (PharMingen, San Diego, CA) that was modified by insertion of a glutathione *S*-transferase coding sequence and a PreScission Protease cleavage site upstream and in frame to the Aurora sequences. Recombinant viruses containing the different recombinant transfer vectors were produced following standard protocols (BaculoGold manual; Life Technologies, Inc., Rockville, MD). For protein production, High5 cells, grown in flasks at 27°C in ultimate serum-free medium (Invitrogen), were infected with each recombinant virus and treated with 500 nmol/L okadaic acid 3 hours before collection. Cells were then collected 42 hours after infection and resuspended in ice-cold lysis buffer [PBS (pH 7.4), 500 mmol/L NaCl, 10% glycerol, 0.2% CHAPS, 20 mmol/L DTT, 1 mmol/L orthovanadate, Complete protease inhibitor cocktail (Roche Diagnostics, Mannheim, Germany)]. After sonication, the protein extract was centrifuged at 33,000 × *g* for 45 minutes. The suspension was loaded onto a glutathione-Sepharose 4 fast flow column (Amersham Biosiences) that was preequilibrated in lysis buffer. Proteins were eluted by on-column cleavage with PreScission Protease according to the manufacturer's instructions (Amersham Biosciences). The purified proteins were stored in stabilizing buffer 50 mmol/L Tris (pH 7.6), 500 mmol/L NaCl, 20% glycerol, 1 mmol/L DTT, protease inhibitors, and 1 mmol/L orthovanadate.

In vitro *kinase assays.* Inhibition of kinase activity by PHA-680632 was assessed using a scintillation proximity assay format. In this assay, the biotinylated substrate is transphosphorylated by the kinase in presence of ATP traced with γ^{33}-ATP. The phosphorylated substrate is then captured using streptavidin-coated scintillation proximity assay beads and the extent of phosphorylation is evaluated by β-counter after a 4-hour rest for the floatation of the beads on a dense 5 mol/L CsCl solution. In particular a peptide derived from the Chocktide sequence (LRRWSLGL) was used as substrate for Aurora A, whereas the optimized peptide Auroratide[1] was employed for Aurora B and C. The assay was run in a robotized format on 96-well plates. The potency of the compound toward Aurora kinases and 29 additional kinases belonging to our Kinase Selectivity Screening panel (35) was evaluated and the relevant IC_{50}s were determined. For each Kinase Selectivity Screening enzyme, the K_ms for ATP and the specific substrate were initially determined and each assay was then run at optimized ATP ([$2K_m$]) and substrate ([$5K_m$]) concentrations. This setting enabled direct comparison of IC_{50}s of PHA-680632 across the Kinase Selectivity Screening panel for the evaluation of its biochemical selectivity.

Analysis of cell proliferation. Cells were seeded at different densities ranging from 5,000 to 15,000 cm^2 in 24-well plate with the appropriate complete medium. After 24 hours, plates were treated with compound and incubated for 72 hours at 37°C in 5% CO_2 atmosphere. At the end of incubation time, cells were detached from each plate and counted using a cell counter (Beckman Coulter, Fullerton, CA). IC_{50}s were calculated using percentage of growth versus untreated control.

Cell cycle analysis. All of the cells in the plates, including cells floating in the medium, were collected and analyzed. Adherent cells were released from the plastic by trypsin treatment and added to the tubes. Cells were washed in PBS and fixed in 70% ethanol in PBS, resuspended in PBS containing RNase A (2 μg/mL) and propidium iodide (5 μg/mL), and incubated for 30 minutes at 37°C. Samples were analyzed by flow cytometry with a FACScan (Becton Dickinson Biosciences, San Jose, CA). Data were analyzed with ModFit LT software (Verity Software House, Topham, ME).

The tumors were excised and minced and a cell suspension was prepared by passing the tumor thrice through a needle. The suspension was centrifuged and the cells were resuspended in CytoPerm and stained with anti-active caspase-3 (BD Biosciences, San Jose, CA) according to the manufacturer's protocol.

RNA interference. For small interfering RNA (siRNA) experiments, the following double-stranded RNA oligonucleotides were used: 5′-AUGCCCUGUCUUACUGUCA-3′ and 5′-GUCCCAGAUAGAGAAG-GAG-3′, specific for Aurora A and B, respectively. GL2 oligonucleotide

[1] L. Rusconi et al., in preparation.

(Dharmacon Research, Inc., Lafayette, CO), which targets the luciferase gene, was used as control. All of the siRNA duplexes were synthesized by Dharmacon and were transfected using Oligofectamine (Invitrogen) according to the manufacturer's recommendations. siRNAs were used at final concentrations of 100 nmol/L.

Immunoblotting. Cell or tissue extracts were prepared in 125 mmol/L Tris-HCl (pH 6.8) and 2% SDS. Samples were sonicated and heated for 5 minutes at 95°C. Protein extract (10 μg), as determined by BCA protein assay (Pierce, Rockford, IL) was loaded on SDS-PAGE. Immunoblot analysis was done using the following antibodies: anti-Aim1 and anti-Iak1 (BD Transduction Laboratories, Franklin Lakes, NJ), anti-phosphorylated histone H3 Ser^{10} (Upstate Biotechnology, Lake Placid, NY), anti-phospho-Aur2 (T288) (Cell Signaling, Danvers, MA), anti-BubR1 (a kind gift from Dr. T.J. Yen, Fox Chase Cancer Center, Philadelphia, PA), anti-active caspase-3 (Chemicon International, Temecula, CA), anti-active caspase-9 (Oncogene, San Diego, CA), anti-Cdk2 (Santa Cruz Biotechnology, Santa Cruz, CA), anti–histone H3 (Abcam, Cambridge, United Kingdom), and anti-γ-tubulin (Sigma). Immunoblotting was done according to standard methods. SuperSignal chemiluminescence kit (Pierce) was used for detection.

Array Scan IV. The Array Scan 4.0 system (Cellomics, Pittsburgh, PA) was used to analyze cells positive for phosphorylation of histone H3 in Ser^{10}. The Array Scan software mitotic index algorithm (Cellomics) was used to calculate the percentage of cells positive for phosphorylation of histone H3 in Ser^{10}. Plates (96 wells) were seeded with 8,000 U2OS cells per well, and on the day after, the cells were treated for 7 hours with 75 ng/mL nocodazole followed by different doses of PHA-680632 for 1.5 hours.

Cells were then fixed in 3.7% formaldehyde (Sigma) for 20 minutes, washed with PBS, and permeabilized with 0.5% Triton X-100 (Sigma) in PBS for 15 minutes. Phosphorylated histone H3 Ser^{10} (40 μL; Cell Signaling) was added to each well at the recommended dilution in PBS containing 1% bovine serum albumin and 0.3% Tween 20 (Sigma) for 1 hour at 37°C. An anti-rabbit primary Cy2-conjugated secondary antibody (Amersham Biosciences) was used for antigen detection.

Immunocytochemistry. Tumors were harvested, formalin-fixed, and paraffin-embedded. Paraffin sections (3 μm) were deparaffinized in xylene, rehydrated in graded ethanol, and transferred to PBS. Sections were placed in citrate buffer (pH 6.0) and thermally processed with two cycles in autoclave "2100 Retriever" (PickCell Laboratories, Amsterdam, the Netherlands). After washing with PBS, endogenous peroxidase was blocked using 3% hydrogen peroxide in PBS for 10 minutes. The tissues were washed with PBS plus 0.01% Tween 20 and incubated for 30 minutes at room temperature with a protein-blocking solution consisting of PBS containing 10% normal goat serum and 0.01% Tween 20. The sections were stained with an anti-phosphorylated histone H3 Ser^{10} polyclonal antibody (Upstate Biotechnology) diluted 1:800 in blocking solution and incubated for 1 hour at room temperature. The samples were rinsed twice with PBS plus 0.01% Tween 20, incubated for 30 minutes at room temperature with Envision rabbit (DAKO, Glastrup, Denmark), rinsed, and incubated for 3 minutes with 3,3′-Diaminobenzidine Plus (DAKO). The sections were then washed and counterstained with hematoxylin. For the bromodeoxyuridine labeling, 2 hours before mice were sacrificed, 100 mg/kg bromodeoxyuridine (Sigma) was injected i.p. Excised tumors were formalin-fixed for 24 hours and paraffin-embedded. The sections were processed as above and stained with a monoclonal antibody specific for bromodeoxyuridine (Becton Dickinson).

Animal efficacy studies. Female Hsd, athymic *nu/nu* mice, ages 5 to 6 weeks (20-22 g), and female severe combined immunodeficient mice were obtained from Harlan (San Pietro al Natisone, Italy). Mouse mammary tumor virus v-Ha-*ras* transgenic mice were originally obtained from Charles River Breeding Laboratories (Wilmington, MA) and maintained in a FVB background.

All animal studies were carried out in compliance with Italian Legislative Decree N.116 dated January 27, 1992 and the European Communities Council Directive N.86/609/EEC concerning the protection of animals used for experimental or other scientific purposes and according to Institutional Policy Regarding the Care and Use of Laboratory Animals. A2780 human ovarian carcinoma and HCT116 colon carcinoma cell lines (American Type Culture Collection) were transplanted s.c. into athymic mice. Mice bearing a palpable tumor (100-200 mm^3) were selected and randomized into control and treated groups. Treatments started 1 day after randomization.

In the HL60 study, female severe combined immunodeficient mice were injected s.c. with 5×10^6 leukemia cells. Treatments started, when tumors were 200 to 250 mm^3 in size.

In the study with mouse mammary tumor virus v-Ha-*ras* transgenic mice with established mammary tumors, compound administration began when mammary tumors had an average volume in the range of 300 to 500 mm^3. In all cases, tumor growth was measured approximately once weekly for 7 weeks and animal weight was measured twice weekly.

Dimensions of the tumors were measured regularly by caliper during the experiments and tumor masses were calculated as described (36). The TGI (%) was calculated according to the equation: % TGI = 100 − (mean tumor weight of treated group / mean tumor weight of control group) × 100. Toxicity was evaluated based on the body weight reduction. Mice were sacrificed when the tumors reached a volume that hampered them, and the gross autopsy findings were reported.

Results

PHA-680632 is a cell cycle inhibitor specific for Aurora kinases. PHA-680632 was identified by the combinatorial expansion of the 1,4,5,6-tetrahydropyrrolo[3,4-*c*]pyrazole scaffold as described previously (ref. 37; Fig. 1A). The specificity of this compound was tested *in vitro* against a broad panel of kinases representative of different kinase families. PHA-680632 was shown to be a potent inhibitor of all three Aurora kinases with IC_{50}s of 27, 135, and 120 nmol/L for Aurora A, B, and C, respectively. The selectivity of PHA-680632 for the Aurora kinases was tested over a panel of 29 additional kinases (Fig. 1B) and the compound was found to be inactive (IC_{50}, >10 μmol/L) on 22 of them. Six kinases in the panel (FLT3, LCK, PLK1, STLK2, VEGFR2, and VEGFR3; Fig. 1B) exhibited a 30- to 200-fold higher IC_{50} compared with Aurora A. The strongest cross-reactivity was seen with FGFR1, although PHA-680632 retained a ~15-fold selectivity for Aurora A (IC_{50} for FGFR1, 390 nmol/L).

We then evaluated the antiproliferative effects of PHA-680632. A panel of 35 exponentially growing cell lines from different tumor types and NHDF were treated for 72 hours with different concentrations of PHA-680632 (Fig. 1C; Supplementary Data 1). PHA-680632 has potent antiproliferative activity in a wide range of cell types with an IC_{50} in the range of 0.06 to 7.15 μmol/L. The antiproliferative effect of our inhibitor was determined by cell counting because inhibition of Aurora kinases induces endoreduplication and gives rise to cells with a DNA content higher than 4N accompanied by an increase of the cell diameter. Conventional standard assays used to measure proliferation [as 3-(4,5-dimethylthiazol-2-yl)-2,5-diphenyltetrazolium bromide, sulforhodamine B, or ATP level evaluation] give misleading results and direct cell count as a readout for Aurora kinase inhibition allows a more appropriate determination of IC_{50}s and comparison of compounds.

PHA-680632 can cause polyploidy in tumor cells. Inhibition of Aurora kinases has been shown to generate polyploid cells as a consequence of DNA synthesis in the absence of cytokinesis (32). We evaluated the effects of PHA-680632 on the cell cycle

A

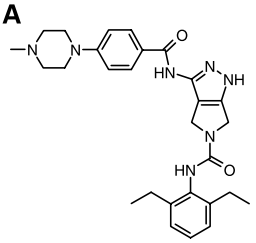

B

Kinase	IC_{50} (nM)
Aurora A	27
Aurora B	135
Aurora C	120
FGFR1	390
FLT3	820
LCK	1950
PLK1	780
STLK2	5500
VEGFR2	1920
VEGFR3	1000

C

Cell lines	IC_{50} (μM)
C33A	0.32
HeLa	0.41
HCT116	0.06
HT29	1.17
LOVO	0.56
A549	0.62
MCF7	0.29
A2780	0.11
U2OS	1.56
DU145	0.62
U937	0.07
HL60	0.13
NHDF	0.41

Fig. 1. PHA-680632 is a selective Aurora inhibitor that blocks proliferation of several tumor cell types. *A,* chemical structure of PHA-680632, a derivative of a 1,4,5,6-tetrahydropyrrolo[3,4-*c*]pyrazole scaffold. *B,* IC_{50}s of PHA-680632 against a panel of protein kinases. PHA-680632 was not active (IC_{50}, >10 μmol/L) against the following kinases: BUB1, CDC7, CDK2/CycA, CHK1, CK2, CMET, EGFR, ERK2, GSK3β, IGFR1, IKK1, IKK2, IR, LYN, MAPKAPK2, NIM1, PAK4, PKAα, PKBα, PKCβ, SULU1, and ZAP70. *C,* antiproliferative effect of PHA-680632 in a panel of human cell lines. The complete panel can be found in Supplementary Data 1. Mean of two or more independent dose-response curves.

by flow cytometry in NHDF as well as in several cancer cell lines, including HCT116, A2780, HL60, and HeLa cells. Cells were treated with increasing concentrations of PHA-680632 for 24, 48, and 72 hours (Fig. 2; Supplementary Data 2A). The cell lines respond with different kinetics and reach a saturation status at different doses. In Fig. 2A, we show comparison between HCT116 and NHDF treated for 24 hours. Whereas the tumor cell line HCT116 rapidly enters endoreduplication at low doses of PHA-680632, the NHDF require higher doses to accumulate in a 4N DNA content stage and do not reach polyploidy within the 24 hours of treatment. The increase in DNA content goes along with an increase in cell diameter (e.g., the percentage of HCT116 cells with a diameter between 15 and 25 μm increases from 14% in the control cells up to 90% in the treated cells). (The average diameter of HCT116 cells is 12 μm).

We then measured the effect of PHA-680632 over time to exclude the possibility that the differential responses seen are due to the different cycling time of the cells. The cell lines were followed for 24, 48, and 72 hours at different doses and Fig. 2B and Supplementary Data 2B show the profiles for each cell line tested at the dose for which saturation was reached in the titration experiment. The more sensitive cell lines, which displayed polyploidy already at 24 hours, do not change behavior, with the exception of HL60 cells that display massive cell death over time (Supplementary Data 2B). On the contrary, increasing the time, it was possible to see some polyploidy also in HeLa cells, whereas NHDF stayed blocked in the cell cycle even when treated at higher doses for 72 hours (Fig. 2B; Supplementary Data 2B). We then tested the ability of the cells to recover after drug washout (Fig. 2C). HCT116 cells and NHDF were treated with 0.5 μmol/L PHA-680632 for 40 hours, and cells were replated in drug-free medium and collected for analysis 6 days after the replating. As shown in Fig. 2C, after treatment, the majority of the HCT116 cells are in a polyploid stage, whereas NHDF are mainly in the G_2-M phase of the cell cycle. At 6 days after replating, the DNA profile shows that the NHDF are back to normality (with ~90% in cell number of the untreated cells), whereas for the tumor cells there is a very low number of cells (3% of the untreated), showing only partial recovery of cells associated with an abnormal DNA profile. These data strongly suggest a selective effect of PHA-680632 on different cell types spanning from induction of polyploidy to a 4N cell cycle block and may implicate that PHA-680632 might be selectively toxic to some tumor cells.

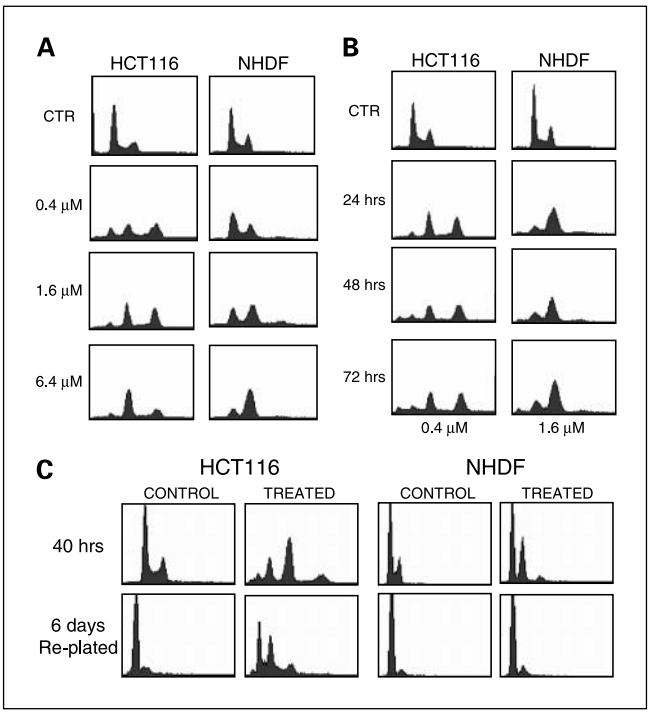

Fig. 2. Effect of PHA-680632 on the cell cycle and comparison between NHDF and a tumor cell line (HCT116). *A,* cells were treated for 24 hours with PHA-680632 at the indicated concentrations. After treatments, cells were collected and analyzed by flow cytometry. *B,* cell cycle analysis of HCT116 and NHDF treated with PHA-680632 at the indicated concentrations at 24, 48, and 72 hours of treatment. *C,* HCT116 and NHDF were treated with 0.5 μmol/L PHA-680632 for 40 hours. The remaining cells were collected and replated to follow regrowth up to 6 days. After treatments, cells were collected and analyzed by flow cytometry.

PHA-680632 cell treatment induces phenotypes similar to Aurora A or B depletion. To better explore the mechanism of action of PHA-680632, we compared the effect of the inhibitor on cells with siRNA down-regulating Aurora A or B. We designed several siRNA oligonucleotides corresponding to Aurora A and B and tested them for different times to choose the optimal conditions to reduce Aurora mRNA and protein. A typical result is shown in Fig. 3A, where HeLa cells were transfected with Aurora A or B oligonucleotides and after 48 hours showed a good reduction of the proteins in comparison with untreated cells or cells transfected with control siRNA oligonucleotides.

HeLa cells depleted either of Aurora A or B showed different phenotypes with cells accumulating with different DNA content. Aurora A siRNA promotes apoptosis as shown by an increase of the sub-G_1 cell population (Fig. 3B) and by the presence of active caspase-9 and caspase-3 measured by Western blot. Aurora A siRNA also does not inhibit histone H3 phosphorylation (Fig. 3A). On the contrary, depletion of Aurora B does not activate caspases but inhibits histone H3 phosphorylation. Moreover, Aurora B siRNA leads to an increase in 4N DNA content, and over the time, the percentage of cells with a DNA content higher than 4N is seen (Fig. 3B). Using the inhibitor, the morphologic effects on cells recall the ones obtained by depleting Aurora B as confirmed by phase-contrast microscopy (Fig. 3C). However, also at the molecular level, the induction of active caspase-9 and caspase-3 (Fig. 3A) is observed, which is compatible with Aurora A inactivation. This effect was measured also *in vivo* in tumor xenografts of treated mice (Fig. 4).

Inhibition of histone H3 phosphorylation due to Aurora B siRNA is in good agreement with the published data (38). All the reported Aurora inhibitors to date have shown modulation of histone H3 phosphorylation at Ser^{10}. Accordingly, HeLa cells treated with 2 μmol/L PHA-680632 for 24 hours also show a strong reduction of the phosphorylation of histone H3 in Ser^{10} (Fig. 3A), confirming the activity of our compound on Aurora B. Moreover, as shown in Fig. 3D, when HeLa cells are treated for 1 hour with PHA-680632 at concentrations ranging between 0.1 and 20 μmol/L, the compound clearly inhibits both Aurora A autophosphorylation at T288 (39) and Aurora B–mediated phosphorylation of histone H3 as expected for a dual Aurora kinase inhibitor (40).

A reduction in phosphorylation of BubR1, which is phosphorylated in response to spindle damage, was shown with siRNA experiments targeting Aurora B and also using Aurora kinase inhibitors (32, 40). In fact, upon treatment of HeLa cells with nocodazole, it is possible to observe a band shift of BubR1 due to phosphorylation (Fig. 3E, *arrow*). In the presence of PHA-680632, disappearance of the band corresponding to phospho-BubR1 is observed, suggesting that Aurora B–mediated phosphorylation of BubR1 is also inhibited (Fig. 3E). In summary, the drug-induced phenotypes are consistent with inhibition of Aurora A and B.

PHA-680632 suppresses tumor growth in animal models. The effect of PHA-680632 on tumor growth was evaluated in human tumor cell xenografts models and in syngeneic models in mouse and rat (Fig. 4; data not shown). PHA-680632 was initially evaluated in the HL60 human acute myelogenous leukemia xenograft model in a dose-finding study. After i.v. administration, at three dose levels (15, 30, and 45 mg/kg b.i.d. consecutively for 5 days), a significant TGI was observed as shown in Fig. 4A (*top*). The 45 mg/kg dose resulted in 85% of TGI without signs of toxicity. In the A2780 human ovarian carcinoma model (Fig. 4A, *middle*), the dose of 60 mg/kg i.v. b.i.d. for 5 days showed potent tumor inhibition, reaching 78% of TGI compared with the vehicle-treated controls. A more prolonged exposure to PHA-680632 was tested in the HCT116 colon carcinoma xenograft, administering the compound i.p. t.i.d. for 12 days. The treatments were also in this case well tolerated and TGI was 75% compared with controls (Fig. 4A, *bottom*).

PHA-680632 efficacy was then evaluated in a syngeneic breast cancer model where tumors arose through a transgenic oncogene. PHA-680632 inhibited growth of activated *ras*-driven mammary tumors in mouse mammary tumor virus v-Ha-*ras* transgenic mice, which exhibit many characteristics of human breast tumors, including spontaneous development and local invasiveness. PHA-680632 treatment of mice bearing established tumors resulted in complete tumor stabilization and partial regression (Fig. 4B). Comparable results were also obtained administering PHA-680632 to rats harboring 7,12-dimethylbenz(*a*)anthracene-induced mammary carcinomas (data not shown), showing the effectiveness of this agent against syngeneic models of mammary cancers arising from either oncogene overexpression or carcinogen exposure. Moreover, histologic analysis of A2780 xenografts at day 10 after treatment (30 mg/kg t.i.d) showed an increase in cellular and nuclear size and the appearance of multinucleated cells similar to the phenotype obtained with cell lines in tissue culture (Supplementary Data 3). Proliferation of tumor cells *in vivo* as measured by bromodeoxyuridine incorporation in the same xenograft model showed also a significant reduction after 5 days treatment with PHA-680632 (30 mg/kg b.i.d.). In HL60 xenografts, we observed in addition an ~3-fold increase in apoptosis as measured by caspase-3 staining (Supplementary Data 3). In summary, these observations *in vivo* confirm the effect of the compound observed *in vitro* and provide useful tools to follow activity of the inhibitor *in vivo*.

***Phosphorylation of histone H3 at Ser^{10} is a biomarker that allows PHA-680632 activity to be monitored* in vitro *and* in vivo.** Inhibition of the phosphorylation of histone H3 at Ser^{10} caused by our Aurora inhibitor was confirmed in several cell lines. Using Array Scan 4.0 System, we were able to calculate an IC_{50} for this inhibition, which is 0.39 μmol/L in U2OS cells (Fig. 5A). U2OS are relatively resistant to polyploidy induction when treated with PHA-680632 for 24 hours with several doses of the inhibitor as shown by flow cytometry (Fig. 5B). Time-course experiments on U2OS cells treated with PHA-680632 showed that the inhibitory effect on the phosphorylation of the histone H3 is very fast: already after 15 minutes of treatment, it is possible to see the disappearance of the signal (Fig. 5C). This response makes histone H3 phosphorylation a fast and sensitive readout for targeting Aurora B. We tested whether this modulation can also be observed *in vivo* using tissues of mice treated with PHA-680632. Nude mice bearing A2780 xenografts were treated i.v. bolus with vehicle only or 60 mg/kg PHA-680632. Animals were sacrificed 30 minutes, 2 hours, 8 hours, and 24 hours after treatment. In bone marrow and tumors, phosphorylation of histone H3 was analyzed by immunohistochemistry and Western blot (Fig. 6A and B). In both tissues, it was possible to observe a strong reduction of

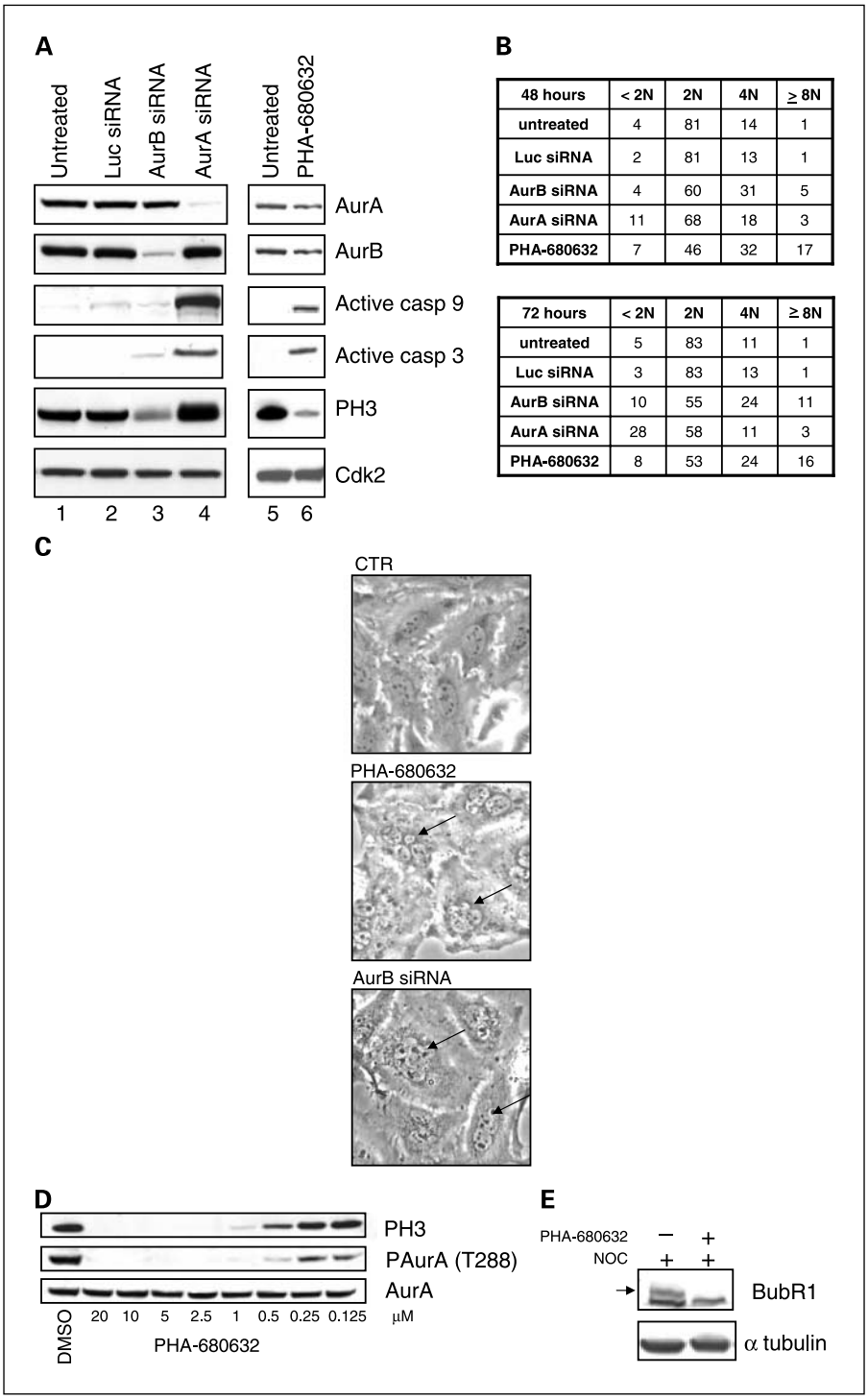

48 hours	< 2N	2N	4N	≥ 8N
untreated	4	81	14	1
Luc siRNA	2	81	13	1
AurB siRNA	4	60	31	5
AurA siRNA	11	68	18	3
PHA-680632	7	46	32	17

72 hours	< 2N	2N	4N	≥ 8N
untreated	5	83	11	1
Luc siRNA	3	83	13	1
AurB siRNA	10	55	24	11
AurA siRNA	28	58	11	3
PHA-680632	8	53	24	16

Fig. 3. Phenotype of down-regulating Aurora kinases by siRNA or treatment with PHA-680632. *A,* Western blot analysis of extracts prepared from HeLa cells 48 hours after transfection or after compound treatment. *Lanes 1* and *5,* nontransfected cells; *lane 2,* control siRNA; *lane 3,* Aurora B siRNA; *lane 4,* Aurora A siRNA; *lane 6,* 2 μmol/L PHA-680632. Membranes were blotted with the indicated antibodies. An antibody recognizing CDK2 was used as loading control. *B,* percentages of cells with different DNA content were calculated from cell cycle profiles of HeLa cells after transfection with Aurora A or B siRNA for 48 and 72 hours. *C,* phase-contrast microscopy of HeLa cells that were either untreated, treated with 2 μmol/L PHA-680632, or transfected for 72 hours with Aurora B siRNA. *Arrows,* examples of polynucleated cells (~10% of the total culture). *D,* Western blot analysis of HeLa cells treated for 1 hour with PHA-680632 at the indicated concentrations. Activity on Aurora A autophosphorylation (T288) and Aurora B–mediated phosphorylation on histone H3 (S^{10}). *E,* Western blot analysis of HeLa cells treated with nocodazole (9 hours at 75 ng/mL) in the absence (*left lane*) or presence (*right lane*) of 2 μmol/L PHA-680632 for the last 2 hours. Membranes were blotted with the indicated antibodies. *Arrow,* band shift associated with phosphorylation of BubR1.

this phosphorylation, although the kinetics were slightly different in the two organs possibly due to tissue penetration or retention of the compound. In both tissues, the effect starts to disappear 8 hours after treatment (Fig. 6), compatible with the half-life of the compound, which is ~70 minutes in mouse plasma. We are currently working on a pharmacokinetic/pharmacodynamic model to correlate efficacy with degree and time of biomarker modulation because the duration of the modulation is a critical factor for efficacy. Effects on histone H3 phosphorylation were also studied in human primary cells from leukemia patients. Total WBC from peripheral blood or bone marrow aspirates of patients with leukemia were purified. Cells were plated and treated with PHA-680632 or with nocodazole that was used as control to confirm that cells were cycling, because it blocks cells in G_2-M and gives a strong increase in the phosphorylation of histone H3. In 6 of 18 cases that responded to nocodazole treatment, we observed an inhibition of the phosphorylation of histone H3 when treated

with PHA-680632. An example of a responsive sample is shown in Fig. 6C. We also measured a massive cell death in the treated samples, but it was not possible to quantify the data considering the high ratio of spontaneous apoptosis in this type of cells once put into culture.

In summary, these data strongly indicate that phosphorylation of histone H3 at Ser^{10} is a good candidate as a biomarker for preclinical and clinical studies of an Aurora kinase inhibitor and to give an indication for plasma target concentrations to be reached in a clinical trial.

Discussion

PHA-680632 was developed as an ATP competitive compound with high activity on Aurora kinases. The compound showed minor cross-reactivity with other kinases tested. One of the cross-reactivities involves FGFR1 and its inhibition by PHA-680632 *in vivo* may contribute to the overall antitumor activity displayed by the compound. For example, the recently described Aurora inhibitor VX-680 (34) inhibits all the Aurora kinases and FLT3 tyrosine kinase [$K_{i(app)}$, 30 nmol/L], which is aberrantly expressed in a large percentage of acute myelogenous leukemia patients. However, for both compounds, the dominant cellular phenotype, as detected by the cell cycle profile, is compatible with an Aurora kinases mode of action (4N and polyploidy) and, in case of PHA-680632, not with inhibition of FGFR1.

Different cells were treated with PHA-680632 showing differences in the cellular response as reflected in the cell cycle profiles. We did not find a correlation between sensitivity of cells in the proliferation assay and the mRNA expression levels of the Aurora kinases within the cell lines analyzed thus far. Differences in sensitivity and type of response might rather be associated with different genetic backgrounds among the cell lines. For instance, HCT116 cells seem to be highly sensitive (IC_{50}, 60 nmol/L) and also readily go to polyploidy and cannot revert the phenotype after drug withdrawal (Fig. 2C). This could be explained considering the fact that HCT116 lack CHFR, a mitotic checkpoint protein (41) recently shown to be involved also in Aurora regulation (42). On the other hand, NHDF that are primary cells with intact checkpoints cannot be brought into polyploidization after treatment even at high doses and long exposures and they are able to return to the normal cell cycle after drug washout. Similar results were obtained with mouse embryo fibroblasts (data not shown).

An involvement of a cell cycle checkpoint in this type of response is supported by the work of Ditchfield et al. (32) describing the Aurora kinase inhibitor ZM447439. They showed different behavior of U2OS cells treated with the inhibitor, in the presence or absence of functional p53, suggesting that Aurora inhibitors might be selectively toxic to tumor cells lacking p53. Indeed, there are evident links between Aurora A and p53 that might correlate with tumor development. It was reported that p53 interacts with Aurora A and suppresses its oncogenic activity in a transactivation-independent manner (24). It was also shown that p53 is phosphorylated by Aurora A. This phosphorylation can promote degradation of p53 (Ser^{315}; ref. 25) or can cause suppression of p53 transcriptional activity (Ser^{215}; ref. 26). Moreover, Aurora A overexpression has been correlated with mutations in p53 in hepatocellular carcinomas and tumors

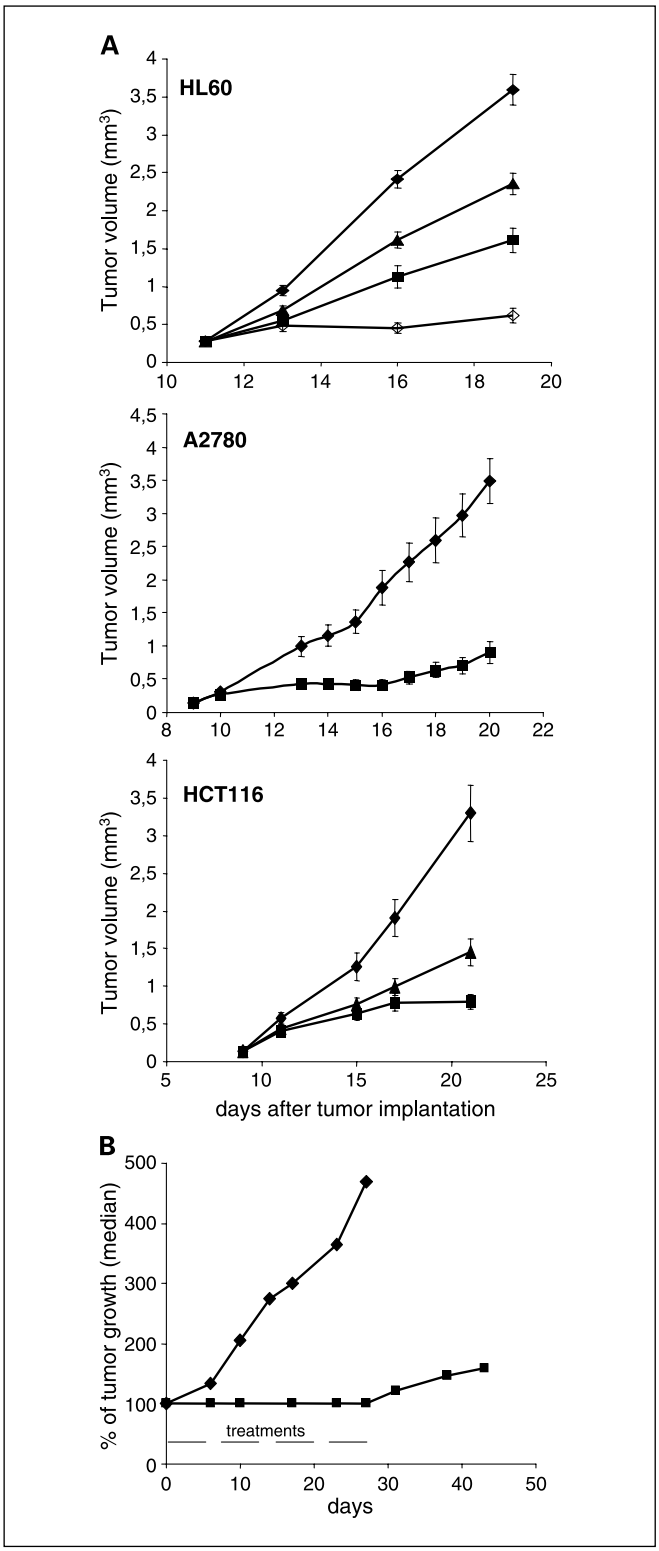

Fig. 4. PHA-680632 suppresses tumor growth in animal models. *A, top,* HL60 tumors were treated i.v. b.i.d. from days 11 to 15 with vehicle (♦) or PHA-680632 at 15 (▲), 30 (■), or 45 (◇) mg/kg. *Middle,* A2780 ovarian carcinoma tumors were treated i.v. b.i.d. from days 9 to 13 with vehicle (♦) or PHA-680632 at 60 mg/kg (■). *Bottom,* HCT116 colon carcinoma tumors were treated i.p. t.i.d. from days 9 to 20 with vehicle (♦) or PHA-680632 at 15 (▲) or 30 (■) mg/kg. *B,* mouse mammary tumor virus v-Ha-*ras* mammary carcinoma established tumors were treated i.p. t.i.d with vehicle (♦) or PHA-680632 at 45 mg/kg (■) followed by 2 days off treatment, repeated for four cycles.

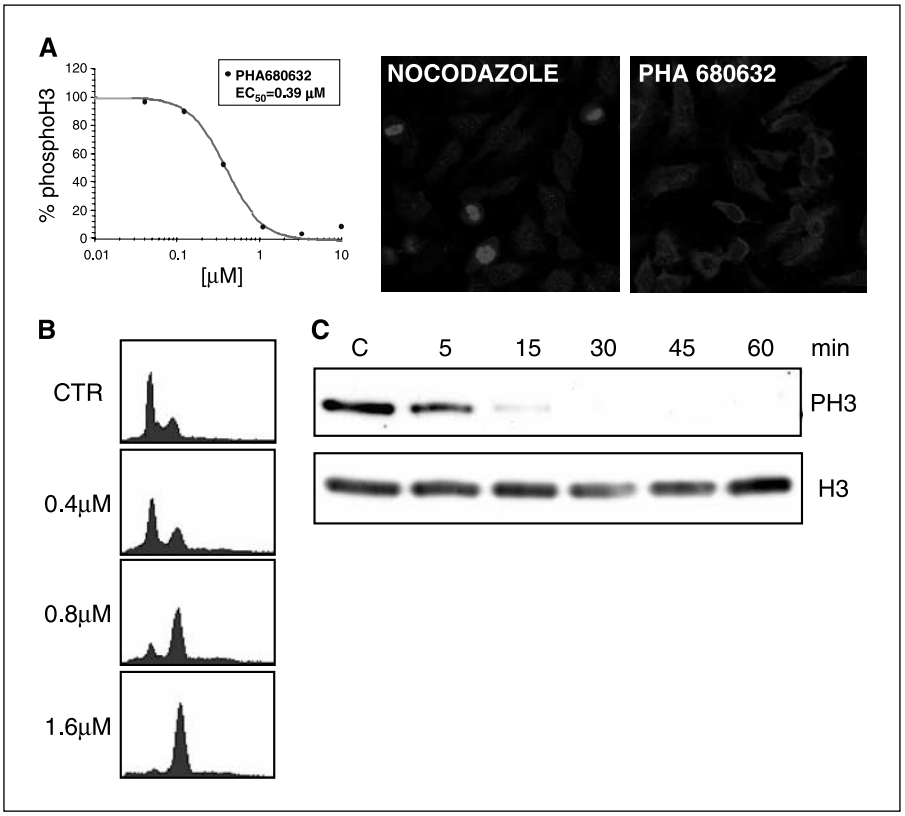

Fig. 5. Kinetics of inhibition of the phosphorylation of histone H3. *A,* Array Scan IV analysis of phosphorylation of histone H3 on U2OS cells treated for 7 hours with 75 ng/mL nocodazole followed by different doses of PHA-680632 for the last 1.5 hours. *B,* cell cycle profiles of U2OS cells treated for 24 hours at the indicated doses of PHA-680632. *C,* Western blot analysis of phosphorylated histone H3 of U2OS cells treated with 5 μmol/L PHA-680632 and collected at the indicated time points.

with both features had the worse prognosis (20), indicating a cooperative effect on tumor formation.

The thus far described Aurora inhibitors, which hit all Aurora kinases, induce a cellular phenotype comparable with the one described here for PHA-680632 and are identical to inactivation of Aurora B alone. This is supported by a recent publication (40), whereby siRNA experiments targeting simultaneously Aurora A and B, resulted in a phenotype comparable with Aurora B siRNA alone, suggesting that inactivation of Aurora B bypasses Aurora A functions in mitosis.

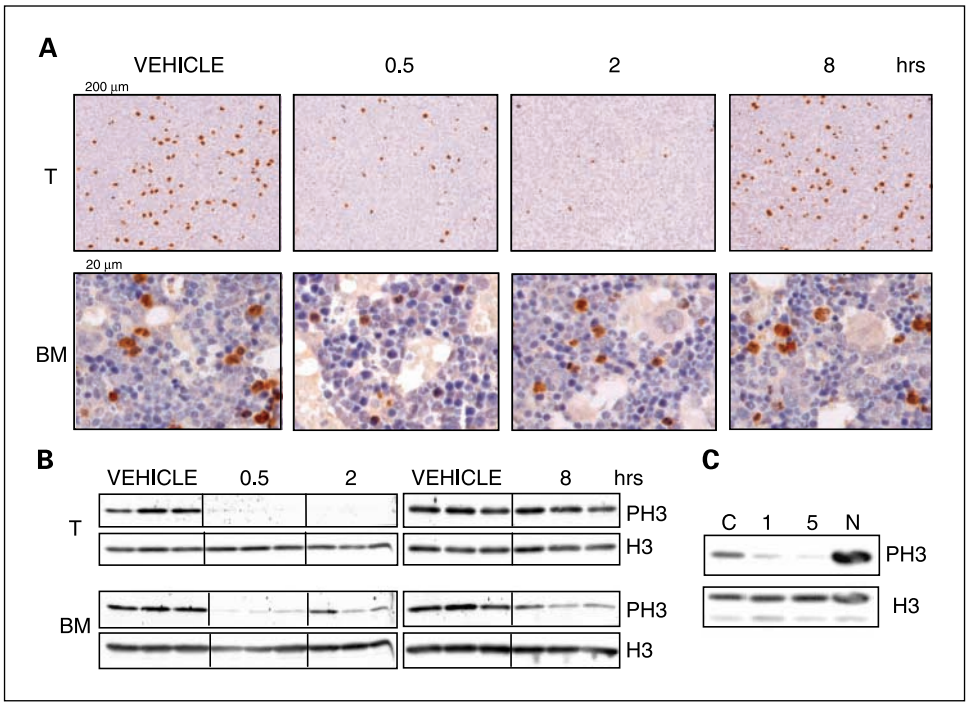

Fig. 6. *In vivo* evaluation of phosphorylated histone H3 modulation. *A,* immunohistochemical staining of phosphorylated histone H3 antigen in tumor (*T*) or bone marrow (*BM*) of mice bearing A2780 xenograft treated i.v. with vehicle only or 60 mg/kg PHA-680632. Animals were sacrificed after treatment at the indicated times. *B,* Western blot analysis of phosphorylated histone H3 (*PH3*) in the same sample described above. Results for three mice that are representative of a group of five. *C*, Western blot analysis of total WBC from an acute myelogenous leukemia patient treated *in vitro* with either nocodazole (75 ng/mL) or 1 μmol/L or 5 μmol/L PHA-680632 for 24 hours. C, control.

Originally, Aurora A and B kinases have been implicated in phosphorylation of histone H3 *in vitro* and *in vivo* (43), but Aurora B seems to be the preferential histone H3 kinase. This modification, which is conserved from yeast to vertebrates, is carried out by Ipl1 in budding yeast (44) and the Aurora B homologue in other organisms, such as *Caenorhabditis elegans* (44) and *Drosophila melanogaster* (45). PHA-680632 is a potent inhibitor of the phosphorylation of histone H3. We were able to measure modulation of the phosphorylation status of histone H3 *in vivo* in different tissues, including bone marrow (Fig. 6) and skin. This property suggests the use of histone H3 phosphorylation as a specific biomarker for a readout of Aurora kinase B in clinical samples. Effects on histone H3 phosphorylation were also seen in human primary cells derived from leukemia patients and we were able to see an inhibition of the phosphorylation of histone H3 when treated with PHA-680632. Interestingly, in a recent publication (46), it has been shown that phosphorylation of histone H3 at Ser^{10} might be required for inducing neoplastic cell transformation, suggesting that inhibition of this phosphorylation could be directly involved in the antitumoral activity that we observed.

A growing number of Aurora kinase inhibitors are in development and first compounds have entered the clinic (29). All the described inhibitors have similar effects on cells, typically mimicking genetic depletion of Aurora B, but they might differ in potency against all three Aurora kinases and specificity against other kinases. PHA-680632 shows the same features consistent with a potent Aurora B inhibitor, although we show also evidence for inhibition of Aurora A. We are currently undertaking experiments to better understand the mechanism of action of our compound during different stages of mitosis and to understand the molecular basis for the differential responses observed in different cell lines. The answer to whether it is better to inhibit Aurora A or B alone or in combination will become clearer once results on selective inhibitors are available. This will be important in a clinical context to minimize potential toxic effects and to identify the appropriate patient population to be treated. For this purpose, it will be useful to compare activities of single and multiple Aurora kinase inhibitors, because these compounds might have different cellular effects. For example, a specific inhibitor of Aurora A would be expected to give an arrest or delay in G_2-M associated with defects in centrosome number, spindle formation, and, consequently, an increase in apoptosis.

Acknowledgments

We thank our colleagues from the Cell Bank, Experimental Therapy Unit, and Toxicology Department of Nerviano Medical Sciences S.r.l. for their contributions and Drs. Porta and Bianchi (Institute of Internal Medicine and Medical Oncology, IRCCS Policlinico San Matteo, Pavia, Italy) and Drs. Brando and Longo (Laboratory of Transplant Immunology and Hematologic Diagnosis, Hospital Niguarda Ca' Granda, Milan, Italy) for providing patient samples.

References

1. Carmena M, Earnshaw WC. The cellular geography of aurora kinases. Nat Rev Mol Cell Biol 2003;4:842–54.
2. Andrews PD, Knatko E, Moore WJ, et al. Mitotic mechanics: the auroras come into view. Curr Opin Cell Biol 2003;15:672–83.
3. Castro A, Vigneron S, Bernis C, Labbe JC, Prigent C, Lorca T. The D-box-activating domain (DAD) is a new proteolysis signal that stimulates the silent D-box sequence of Aurora-A. EMBO Rep 2002;3:1209–14.
4. Littlepage LE, Ruderman JV. Identification of a new APC/C recognition domain, the A box, which is required for the Cdh1-dependent destruction of the kinase Aurora-A during mitotic exit. Genes Dev 2002;16:2274–85.
5. Castro A, Arlot-Bonnemains Y, Vigneron S, Labbe JC, Prigent C, Lorca T. APC/Fizzy-related targets Aurora-A kinase for proteolysis. EMBO Rep 2002;3:457–62.
6. Honda K, Mihara H, Kato Y, et al. Degradation of human Aurora2 protein kinase by the anaphase-promoting complex-ubiquitin-proteasome pathway. Oncogene 2000;19:2812–9.
7. Bischoff JR, Anderson L, Zhu Y, et al. A homologue of *Drosophila* aurora kinase is oncogenic and amplified in human colorectal cancers. EMBO J 1998;17:3052–65.
8. Gassmann R, Carvalho A, Henzing AJ, et al. Borealin: a novel chromosomal passenger required for stability of the bipolar mitotic spindle. J Cell Biol 2004;166:179–91.
9. Meraldi P, Honda R, Nigg EA. Aurora kinases link chromosome segregation and cell division to cancer susceptibility. Curr Opin Genet Dev 2004;14:29–36.
10. Ducat D, Zheng Y. Aurora kinases in spindle assembly and chromosome segregation. Exp Cell Res 2004;301:60–7.
11. Marumoto T, Zhang D, Saya H. Aurora-A—a guardian of poles. Nat Rev Cancer 2005;5:42–50.
12. Kimura M, Matsuda Y, Yoshioka T, Okano Y. Cell cycle-dependent expression and centrosome localization of a third human aurora/Ipl1-related protein kinase, AIK3. J Biol Chem 1999;274:7334–40.
13. Sasai K, Katayama H, Stenoien DL, et al. Aurora-C kinase is a novel chromosomal passenger protein that can complement Aurora-B kinase function in mitotic cells. Cell Motil Cytoskeleton 2004;59:249–63.
14. Katayama H, Brinkley WR, Sen S. The Aurora kinases: role in cell transformation and tumorigenesis. Cancer Metastasis Rev 2003;22:451–64.
15. Li D, Zhu J, Firozi PF, et al. Overexpression of oncogenic STK15/BTAK/Aurora A kinase in human pancreatic cancer. Clin Cancer Res 2003;9:991–7.
16. Katayama H, Ota T, Jisaki F, et al. Mitotic kinase expression and colorectal cancer progression. J Natl Cancer Inst 1999;91:160–2.
17. Gritsko TM, Coppola D, Paciga JE, et al. Activation and overexpression of centrosome kinase BTAK/Aurora-A in human ovarian cancer. Clin Cancer Res 2003;9:1420–6.
18. Sakakura C, Hagiwara A, Yasuoka R, et al. Tumour-amplified kinase BTAK is amplified and overexpressed in gastric cancers with possible involvement in aneuploid formation. Br J Cancer 2001;84:824–31.
19. Fraizer GC, Diaz MF, Lee IL, Grossman HB, Sen S. Aurora-A/STK15/BTAK enhances chromosomal instability in bladder cancer cells. Int J Oncol 2004;25:1631–9.
20. Jeng YM, Peng SY, Lin CY, Hsu HC. Overexpression and amplification of Aurora-A in hepatocellular carcinoma. Clin Cancer Res 2004;10:2065–71.
21. Tong T, Zhong Y, Kong J, et al. Overexpression of Aurora-A contributes to malignant development of human esophageal squamous cell carcinoma. Clin Cancer Res 2004;10:7304–10.
22. Zhou H, Kuang J, Zhong L, et al. Tumour amplified kinase STK15/BTAK induces centrosome amplification, aneuploidy and transformation. Nat Genet 1998;20:189–93.
23. Gigoux V, L'Hoste S, Raynaud F, Camonis J, Garbay C. Identification of Aurora kinases as RasGAP Src homology 3 domain-binding proteins. J Biol Chem 2002;277:23742–6.
24. Chen SS, Chang PC, Cheng YW, Tang FM, Lin YS. Suppression of the STK15 oncogenic activity requires a transactivation-independent p53 function. EMBO J 2002;21:4491–9.
25. Katayama H, Sasai K, Kawai H, et al. Phosphorylation by aurora kinase A induces Mdm2-mediated destabilization and inhibition of p53. Nat Genet 2004;36:55–62.
26. Liu Q, Kaneko S, Yang L, et al. Aurora-A abrogation of p53 DNA binding and transactivation activity by phosphorylation of serine 215. J Biol Chem 2004;279:52175–82.
27. Farruggio DC, Townsley FM, Ruderman JV. Cdc20 associates with the kinase aurora2/Aik. Proc Natl Acad Sci U S A 1999;96:7306–11.
28. Du J, Hannon GJ. The centrosomal kinase Aurora-A/STK15 interacts with a putative tumor suppressor NM23-1. Nucleic Acids Res 2002;30:5465–75.
29. Garber K. Divide and conquer: new generation of drugs targets mitosis. J Natl Cancer Inst 2005;97:874–6.
30. Keen N, Taylor S. Aurora-kinase inhibitors as anticancer agents. Nat Rev Cancer 2004;4:927–36.
31. Hauf S, Cole RW, LaTerra S, et al. The small molecule Hesperadin reveals a role for Aurora B in correcting kinetochore-microtubule attachment and in maintaining the spindle assembly checkpoint. J Cell Biol 2003;161:281–94.
32. Ditchfield C, Johnson VL, Tighe A, et al. Aurora B couples chromosome alignment with anaphase by targeting BubR1, Mad2, and Cenp-E to kinetochores. J Cell Biol 2003;161:267–80.
33. Gadea BB, Ruderman JV. Aurora kinase inhibitor ZM447439 blocks chromosome-induced spindle assembly, the completion of chromosome condensation, and the establishment of the spindle integrity checkpoint in *Xenopus* egg extracts. Mol Biol Cell 2005;16:1305–18.
34. Harrington EA, Bebbington D, Moore J, et al. VX-680, a potent and selective small-molecule inhibitor of the Aurora kinases, suppresses tumor growth *in vivo*. Nat Med 2004;10:262–7.
35. Pevarello P, Brasca MG, Amici R, et al. 3-Aminopyrazole inhibitors of CDK2/cyclin A as antitumor agents. 1. Lead finding. J Med Chem 2004;47:3367–80.

36. Simeoni M, Magni P, Cammia C, et al. Predictive pharmacokinetic-pharmacodynamic modeling of tumor growth kinetics in xenograft models after administration of anticancer agents. Cancer Res 2004;64:1094–101.
37. Fancelli D, Berta D, Bindi S, et al. Potent and selective aurora inhibitors identified by the expansion of a novel scaffold for protein kinase inhibition. J Med Chem 2005;48:3080–4.
38. Pascreau G, Arlot-Bonnemains Y, Prigent C. Phosphorylation of histone and histone-like proteins by aurora kinases during mitosis. Prog Cell Cycle Res 2003;5:369–74.
39. Bayliss R, Sardon T, Vernos I et al. Structural basis of Aurora-A activation by TPX2 at the mitotic spindle. Mol Cell 2003;12:851–62.
40. Yang H, Burke T, Dempsey J, et al. Mitotic requirement for aurora A kinase is bypassed in the absence of aurora B kinase. FEBS Lett 2005;579:3385–91.
41. Summers MK, Bothos J, Halazonetis TD. The CHFR mitotic checkpoint protein delays cell cycle progression by excluding cyclin B1 from the nucleus. Oncogene 2005;24:2589–98.
42. Yu X, Minter-Dykhouse K, Malureanu L, et al. Chfr is required for tumor suppression and Aurora A regulation. Nat Genet 2005;37:401–6.
43. Crosio C, Fimia GM, Loury R, et al. Mitotic phosphorylation of histone H3: spatio-temporal regulation by mammalian Aurora kinases. Mol Cell Biol 2002;22:874–85.
44. Hsu JY, Sun ZW, Li X, et al. Mitotic phosphorylation of histone H3 is governed by Ipl1/aurora kinase and Glc7/PP1 phosphatase in budding yeast and nematodes. Cell 2000;102:279–91.
45. Giet R, Glover DM. *Drosophila* aurora B kinase is required for histone H3 phosphorylation and condensin recruitment during chromosome condensation and to organize the central spindle during cytokinesis. J Cell Biol 2001;152:669–82.
46. Choi HS, Choi BY, Cho YY, et al. Phosphorylation of histone H3 at serine 10 is indispensable for neoplastic cell transformation. Cancer Res 2005;65:5818–27.

Clinical Cancer Research

PHA-680632, a Novel Aurora Kinase Inhibitor with Potent Antitumoral Activity

Chiara Soncini, Patrizia Carpinelli, Laura Gianellini, et al.

Clin Cancer Res 2006;12:4080-4089.